

ARTICLE

Supporting Information

The role of water molecules in piezoelectric-like effects in chitosan-based biodegradable films

Alireza Akbarinejad,^{*abc} Holger Fiedler,^d Donn Adam Gito,^{ab} Thomas Loho,^a Peter C. Sherrell,^{ef} Amanda V. Ellis,^e Kean Aw,^g Jadranka Travas-Sejdic,^{bc} and Jenny Malmstrom^{*abc}

Table S1 Previously reported studies on the effect of humidity on piezoelectric output.

Paper Title	Comments	Ref
Moisture-tunable, ionic strength-controlled piezoelectric effect in cellulose nanocrystal films	A change in the d_{33} response of a cellulose nanocrystal film was reported across a humidity range of 5–80%, showing an increase in d_{33} with rising humidity. However, no further characterisation was performed to reveal the underlying mechanisms responsible for this humidity-affected piezoelectric response.	S1
Measurements properties of the dynamic piezoelectric of bone as a function of temperature and humidity?	The paper provides data on d_{12} and d_{13} changes at RH levels of 33%, 55%, and 75%. However, it does not include a clear discussion of how humidity (water content) influences these piezoelectric modes.	S2
Piezoelectric properties of bone as functions of moisture content	The paper measures changes in d_{14} and d_{31} coefficients of bone with changing RH. While it reports a decrease in both d_{14} and d_{31} with increasing humidity, there is no further investigation and discussion about the possible reasons. Additionally, the trend observed between humidity and piezoelectric output is the complete reverse of our observations, suggesting a fundamentally different mechanism at work.	S3
A high-performance, flexible, and dual-modal humidity-piezoelectric sensor without mutual interference	The paper is not about the effect of humidity on piezoelectric response. The piezoelectric component is PVDF (not a biological material), and in fact, they showed that the piezoelectric response from this sensor is independent of humidity.	S4
Sensing–transducing coupled piezoelectric textiles for self-powered humidity detection and wearable biomonitring	Reports a self-powered humidity sensor by embedding a high piezoresponse Sm-PMN-PT ceramic ($d_{33} = \sim 1500 \text{ pC N}^{-1}$) into a moisture-sensitive polyetherimide (PEI) polymer matrix. While the paper shows the effect of humidity on sensor output, it does not study the humidity effect on the piezoelectric properties of a material. The utilised materials are also not biological materials.	S5

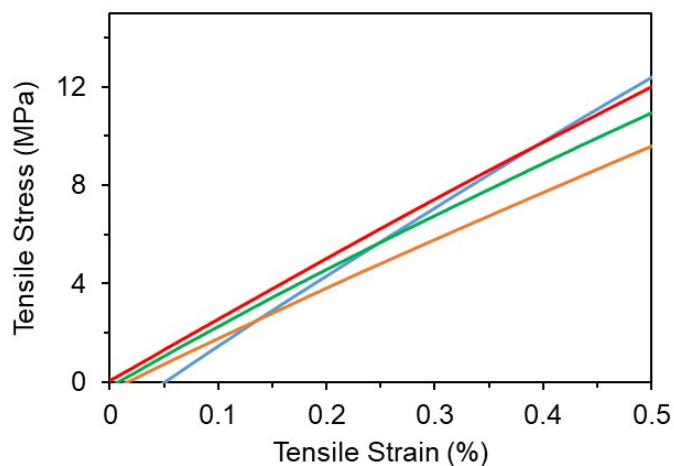


Fig. S1 Tensile stress–strain curves of identical rectangular chitosan films (1.0 cm wide \times 2.0 cm long) tested at a strain rate of 0.1% per second.

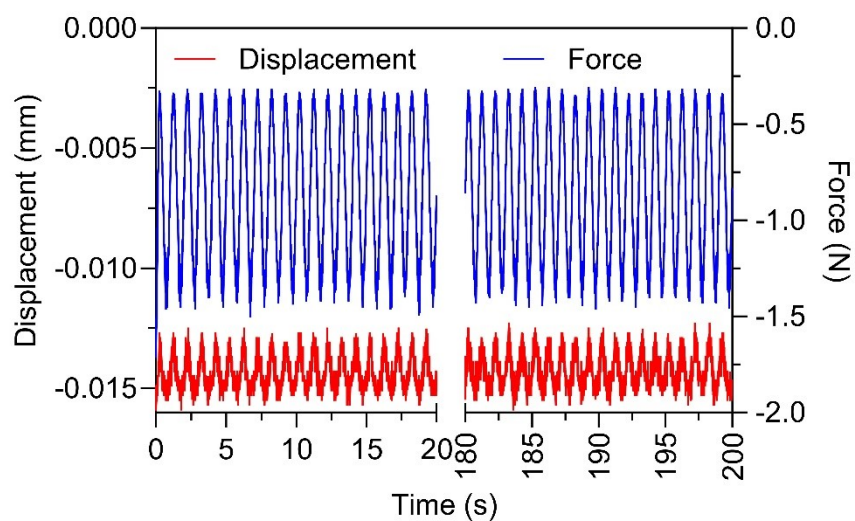


Fig. S2 Cyclic compression response of the chitosan film under an applied force of 1 N for 200 cycles. The force and displacement data are shown for the first and last 20 cycles.

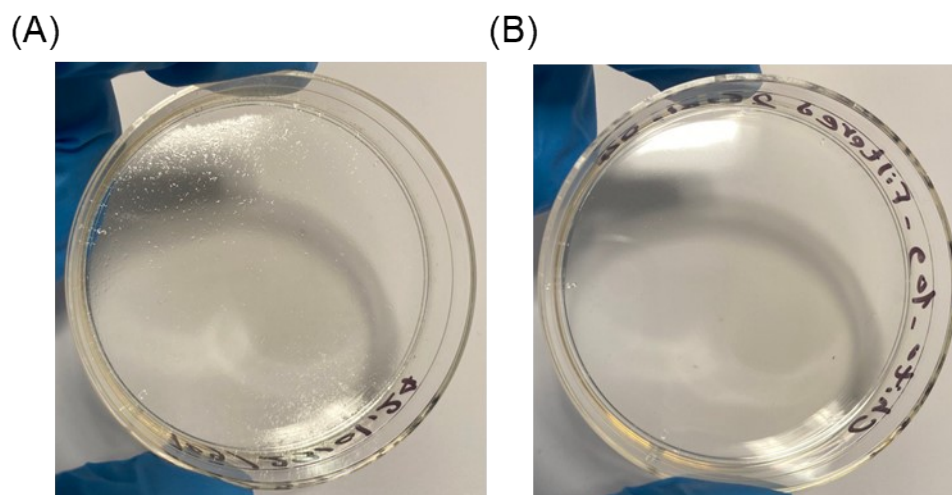


Fig. S3 Photographs of chitosan films prepared using 10 mL of (A) unfiltered and (B) filtered chitosan solutions at an evaporation temperature of 40 °C.

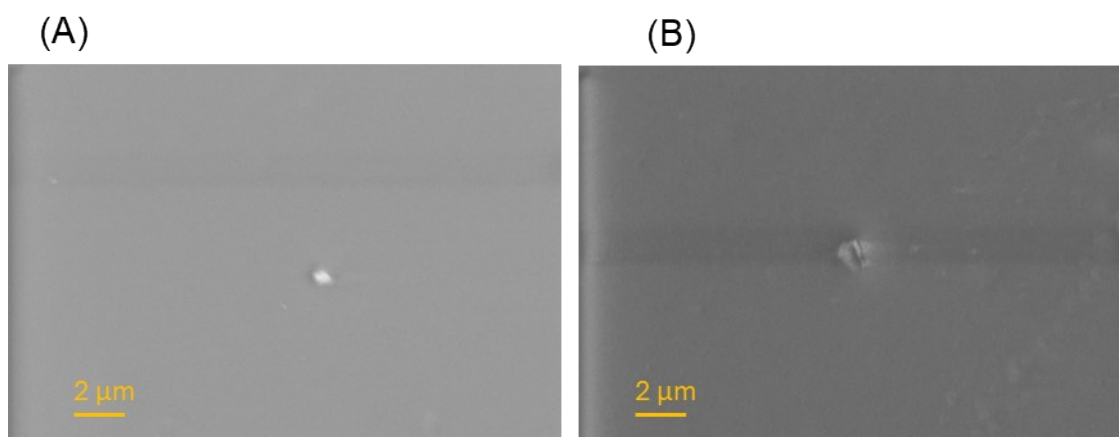


Fig. S4 SEM images of films prepared from (A) unfiltered and (B) filtered chitosan.



Fig. S5 Photograph of the d_{33} meter used in this work.

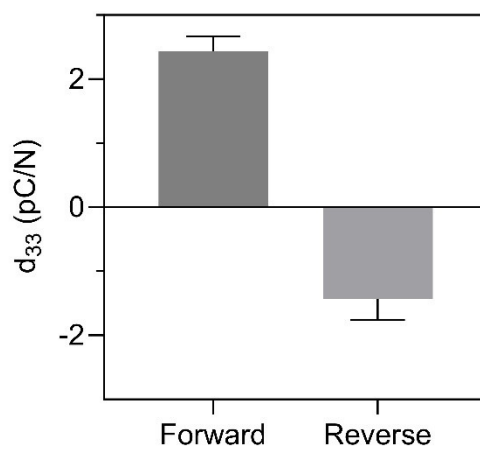


Fig. S6 d_{33} piezoelectric output of chitosan film in forward and reverse modes.

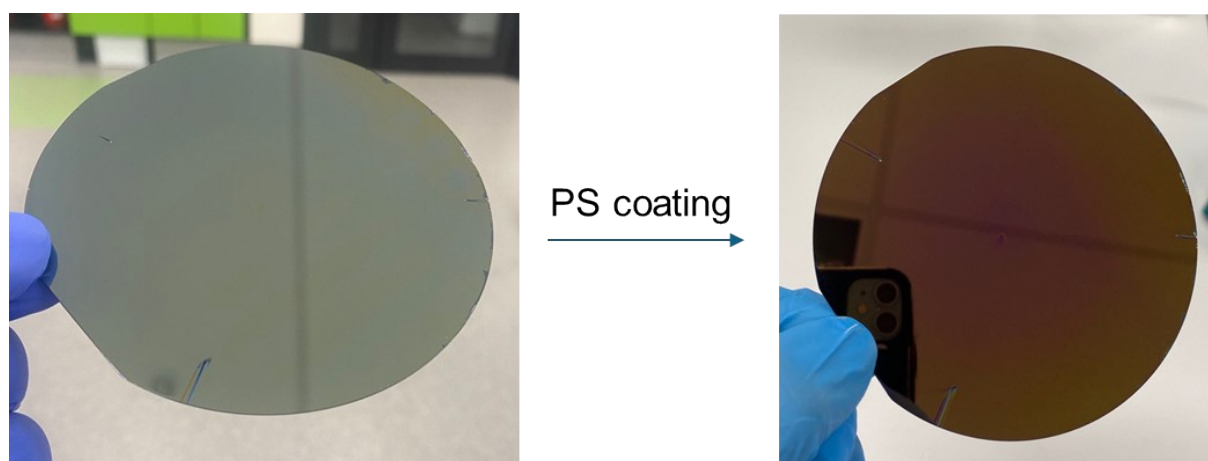


Fig. S7 Photograph of silicon wafer before (left) and after spin coating with polystyrene using a 2 % polystyrene solution in toluene at 3000 RPM for 1 minute (right).

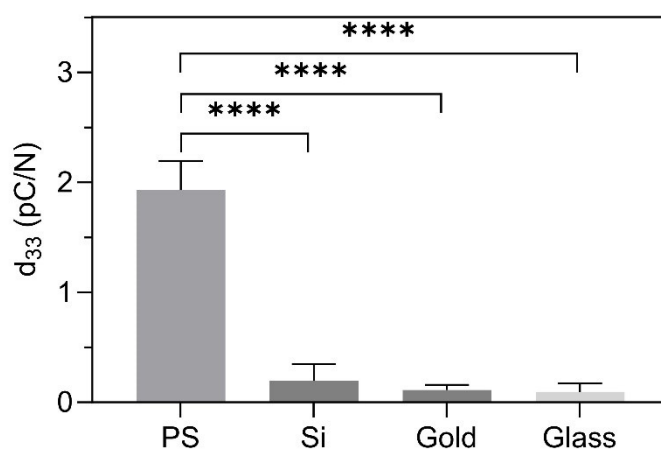


Fig. S8 d_{33} piezoelectric measurements of chitosan films prepared on different substrates. Error bars represent standard deviation based on 2–3 samples, with three measurements per sample ($n = 6–9$). Statistical significance: **** $p < 0.0001$ (based on one-way ANOVA ($\alpha = 0.05$), and Tukey's HSD multi comparison tests).

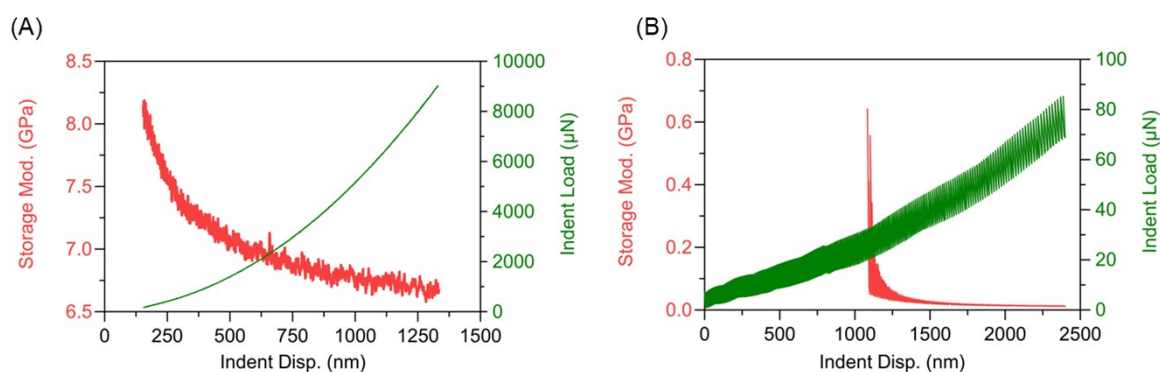


Fig. S9 Storage modulus and indentation load as a function of indentation depth for (A) vacuum-dried chitosan and (B) hydrated chitosan films measured using the continuous measurement of X (CMX) nanoindentation technique.

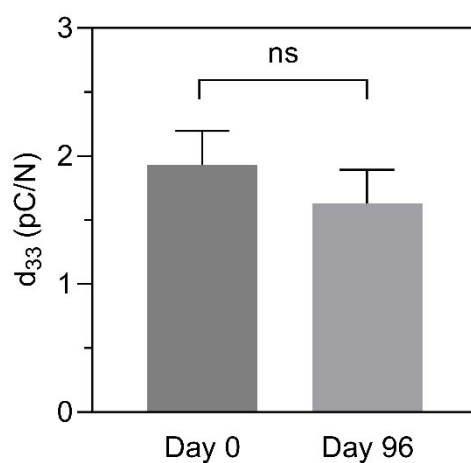


Fig. S10 d_{33} piezoelectric output of ambient chitosan at day 0 and after 96 days (post-fabrication) of storage at ~50–60% RH and 20–22 °C. Error bars represent standard deviation based on 3 samples, with three measurements per sample ($n = 9$).

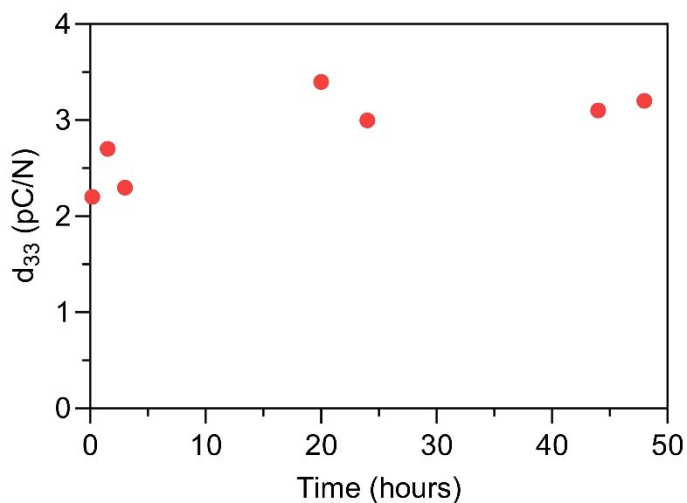


Fig. S11: Time-dependent measurement of the d_{33} coefficient of ambient chitosan films performed on the same location.

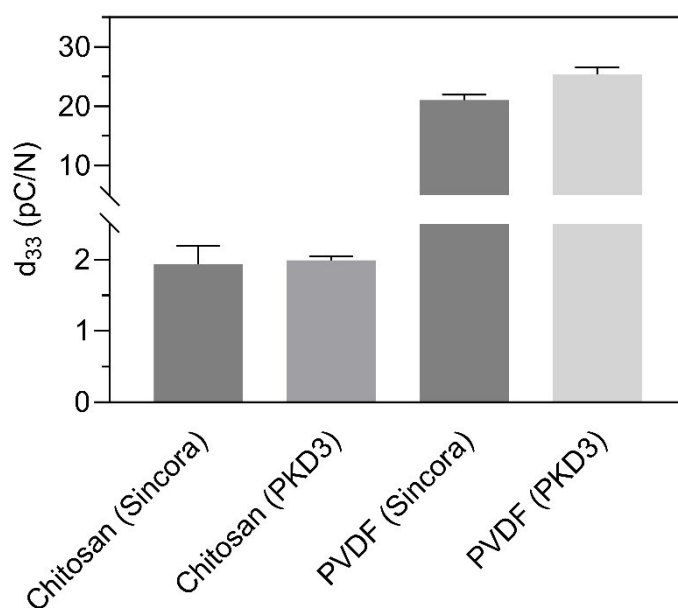


Fig. S12: d_{33} piezoelectric output of ambient chitosan and electrically polled PVDF films measured independently using Sinocera and PKD3 d_{33} meters at a static force of 0.35 N. Error bars represent standard deviation based on 3 samples, with three measurements per sample ($n = 9$).

SI References

- [1] C. Miao, L. Reid, W. Y. Hamad, "Moisture-Tunable, Ionic Strength-Controlled Piezoelectric Effect in Cellulose Nanocrystal Films," *Applied Materials Today* (2021): 24, 101082.
- [2] A. J. Bur, "Measurements of the Dynamic Piezoelectric Properties of Bone as a Function of Temperature and Humidity," *Journal of Biomechanics* (1976): 9, 495.
- [3] G. B. Reinish, A. S. Nowick, "Piezoelectric Properties of Bone as Functions of Moisture Content," *Nature* (1975): 253, 626.
- [4] L. Yang, Q. Liu, M. Li, Y. Liu, X. Li, Q. Liu, T. Zhu, Y. Lu, X. Liu, D. Wang, "A High-Performance, Flexible, and Dual-Modal Humidity-Piezoelectric Sensor Without Mutual Interference," *Sensors and Actuators B: Chemical* (2025): 423, 136778.
- [5] Y. Su, Y. Liu, W. Li, X. Xiao, C. Chen, H. Lu, Z. Yuan, H. Tai, Y. Jiang, J. Zou, G. Xie, J. Chen, "Sensing-Transducing Coupled Piezoelectric Textiles for Self-Powered Humidity Detection and Wearable Biomonitoring," *Materials Horizons* (2023): 10, 842.